Size-dependent oxygen-related electronic states in silicon nanocrystals

J. S. Biteen,[a] N. S. Lewis, and H. A. Atwater
California Institute of Technology, 1200 East California Boulevard, Pasadena, California 91125

A. Polman
California Institute of Technology, 1200 East California Boulevard, Pasadena, California 91125
and FOM Institute for Atomic and Molecular Physics, Kruislaan 407, 1098 SJ Amsterdam, The Netherlands

(Received 20 January 2004; accepted 29 April 2004; published online 17 June 2004)

Silicon nanocrystals embedded in SiO_2 were isolated with a selective etching procedure, and the isolated nanocrystals' excitonic emission energy was studied during controlled oxidation. Nanocrystals having initial diameters, d_0, of $\sim$2.9–3.4 nm showed a photoluminescence (PL) blueshift upon oxidatively induced size reduction, as expected from models of quantum confinement. Oxidation of smaller Si nanocrystals ($d_0 \sim 2.5$–2.8 nm) also initially resulted in a PL blueshift, but a redshift in the PL was then observed after growth of $\sim$0.3 monolayers of native oxide. This decrease in excitonic emission energy during oxidation is consistent with the theoretically predicted formation of an oxygen-related excitonic recombination state. © *2004 American Institute of Physics*. [DOI: 10.1063/1.1765200]

Silicon nanocrystals with diameters, d, less than 5 nm exhibit room temperature visible photoluminescence (PL)[1] due to the recombination of quantum confined excitons.[2] Detailed assessments of the relationship between Si nanocrystal size and band gap using self-consistent tight binding[3] and Quantum Monte Carlo (QMC)[4] methods predict a continuous increase in band gap with decreasing diameter down to diameters less than 1 nm. Experimental measurements have confirmed that the excitonic emission energy of Si nanocrystals increases as the nanocrystal size decreases, but the increase is smaller than that expected theoretically.[3,5,6] This discrepancy suggests the presence of excitonic recombination through a localized electronic state whose energy level lies within the band gap of the smaller Si nanocrystals.

Si nanocrystals are typically embedded in silicon dioxide or surrounded by a native oxide layer, and theoretical models suggest that oxygen-related states at the nanocrystal surface can produce intragap energy levels.[3,4] Wolkin and coworkers evaluated theoretically the effect of a surface silicon-oxygen double bond (Si=O) on the electronic band structure of a Si nanocyrstal.[3] Their semiempirical computations predicted that the energy difference between the conduction and valence bands would increase roughly according to r^{-2}, but their calculations also predicted that, for nanocrystals with $d < \sim 3$ nm, the Si=O bond should produce interface states that lie within the band gap. Puzder *et al.* used QMC calculations for small nanocrystals and interpolated to the bulk band gap with trends from density functional theory to confirm the semiempirical results.[4] More recently, reports of nonlinear optical effects in Si nanocrystal systems have invoked three- or four-level models that require, along with the Si band edges, the presence of deep-lying surface states.[7,8] To test these interface-related excitonic recombination models experimentally, we have used PL spectroscopy to measure the exciton recombination energy of Si nanocrystals in a well-controlled size range, $d \sim 2.5$–3.4 nm, with and without passivation by an oxygen environment.

Ensembles of Si nanocrystals were produced by implantation of 15 keV Si^+ ions to a fluence of 1.3×10^{16} cm^{-2} into 15-nm-thick silicon dioxide films that were grown by thermal oxidation of lightly *p*-doped Si(100). According to SRIM,[9] a Monte Carlo simulation program, such implantations lead to a Gaussian depth distribution of silicon in the SiO_2 matrix and produce a peak excess Si concentration of 15% at a depth of 10 nm. The implanted samples were annealed at 1100 °C for 5 min in Ar. Transmission electron microscopy revealed that this process produced spherical nanocrystals, and atomic force microscopy on HF-etched samples indicated that these nanocrystals had heights (and therefore diameters) of 2–4 nm. The unetched samples were subsequently heated in a forming gas for 30 min at 450 °C to eliminate emission from defect states in the SiO_2 matrix.[10]

PL spectra were acquired under excitation from the $\lambda_{ex} = 458$ nm line of an Ar^+ laser with a power density, P_{ex}, of 60 mW/mm^2, and were collected using a charge-coupled device detector (sensitivity range 200–1100 nm) cooled with liquid nitrogen to −132 °C, in conjunction with a 27.5-cm focal length grating spectrograph. A 510-nm long-pass filter in front of the entrance slit was used to cut off scattered laser illumination, and spectra were integrated for 60 s. The spectrum of a clean silicon wafer was used to remove dark count signatures.

Figure 1 (curve 1-embed) shows the room-temperature PL spectrum of the prepared nanocrystal ensemble. The large spectral width can be ascribed to the distribution of nanocrystal sizes resulting from the nucleation and growth process, as well as to significant homogeneous broadening.[11] The peak PL energy, E_{max}, of 1.60 eV for curve 1-embed, when compared with calculations by Puzder *et al.*,[4] corresponds to a mean nanocrystal diameter of 3.4 nm. To obtain nanocrystal ensembles with slightly smaller mean diameters, the SiO_2 film containing the embedded nanocrystals was annealed for 20 min at 800 °C under O_2. Consistent with prior reports, this oxidizing anneal led to a reduction in the mean nanocrystal diameter.[12] The resulting PL spectrum (curve 2-embed in Fig. 1) was blueshifted by 80 meV, and the corresponding diameter is 3.3 nm.[4]

To obtain even smaller nanocrystals and to isolate them from the SiO_2 matrix, a controlled etching procedure was developed. First, the embedded nanocrystal samples were

[a]Electronic mail: jsbiteen@caltech.edu

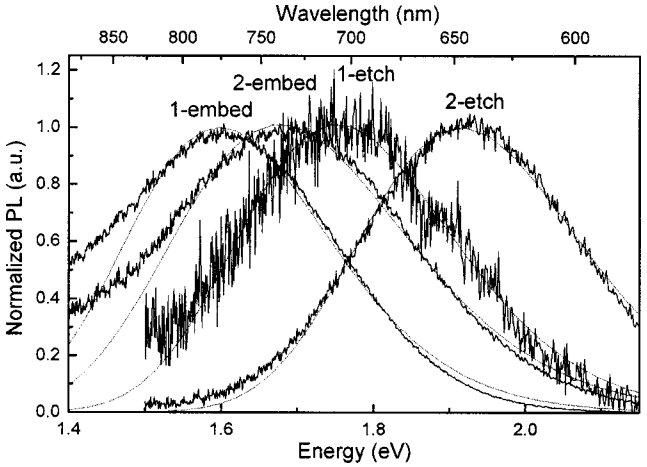

FIG. 1. Normalized room temperature photoluminescence measurements on nanocrystal samples embedded in 15 nm SiO_2 (curves 1-embed and 2-embed) and immediately after etching the SiO_2 (curves 1-etch and 2-etch). The 1-embed, 2-embed, 1-etch, and 2-etch spectra correspond to average nanocrystal diameters of 3.4, 3.3, 3.2, and 2.9 nm, respectively. The absolute intensity of curves 1-embed and 2-embed is ~20 times that of curves 1-etch and 2-etch. $\lambda_{ex}=457.9$ nm, $P_{ex}=60$ mW/mm^2.

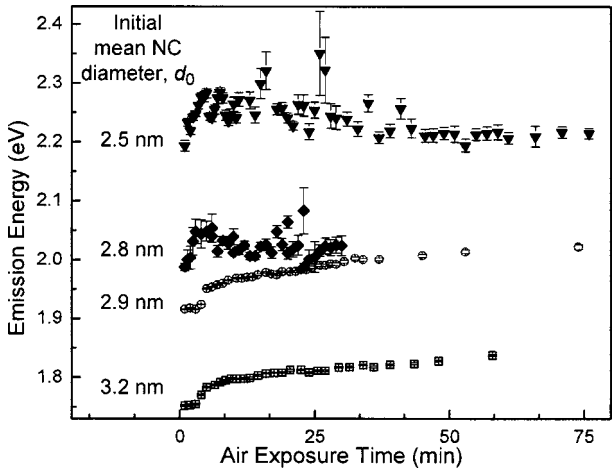

FIG. 2. Time evolution of E_{max} over the course of ambient reoxidation. The samples were etched at $t=0$ min and transferred to an Ar flow chamber in under 1 min, where they remained during PL measurements; excitation and collection were done through a fused silica window. $\lambda_{ex}=457.9$ nm, $P_{ex}=60$ mW/mm^2.

cleaned in a solution of 5:1:1 $H_2O:H_2O_2:NH_4OH$ at 80°C for 10–20 min followed by a rinse in 18 MΩ cm water. The nanocrystals were subsequently removed from the SiO_2 and deposited onto the silicon substrate with a 40-s chemical etch in buffered HF [7.2% HF (aq), 36% NH_4F(aq) v/v]. Care was taken to hold the samples horizontally. These nanocrystals were oxygen-free within the sensitivity of x-ray photoelectron spectroscopy, implying that their surfaces were hydrogen terminated. To prevent oxidation, the nanocrystals were stored under a flow of 99.99% Ar.

After etching, the intensity-normalized PL spectra of both samples (curves 1-etch and 2-etch, Fig. 1) exhibited a 140–150 meV blueshift relative to the spectra of the corresponding embedded samples (curves 1-embed and 2-embed, Fig. 1). The corresponding nanocrystal diameters are 3.2 nm (sample 1-etch) and 2.9 nm (sample 2-etch). The widths of the PL spectra remained constant at 340–360 meV, and the peaks were symmetric for all the measurements discussed in this letter. The reduction in diameter by 0.2–0.4 nm produced by HF etching corresponds to the conversion of approximately two monolayers of Si (one on each side of the nanocrystal) to silicon hydrides as a result of the etch process. The absolute PL intensity for the etched samples was reduced by a factor of ~20 relative to that of their respective embedded precursors, consistent with expectations for a reduction in nanocrystal coverage during the etch. After etching, the average nanocrystal coverage, estimated from the implanted Si fluence, nanocrystal diameter, and PL intensity decrease was in the range of 10^{11}–10^{12} cm^{-2}, i.e., one nanocrystal per 30–100 nm^2 of substrate area. The intensity stayed constant with time in air.

To examine the effect of oxygen on the emission, samples were subjected to short periods (30 s) of *in situ* oxidation in air (21–22°C, 30–35% humidity). To minimize pump-induced photooxidation, the nanocrystal oxidation was performed in the dark. After each oxidation step, the sample chamber was refilled with Ar and PL data were recorded. Figure 2 depicts the resulting evolution of E_{max}, as determined from Gaussian fits to PL spectra, for four sets of samples as a function of the oxidation time in air.

The $d_0=3.2$ and 2.9 nm samples correspond to curves 1-etch and 2-etch in Fig. 1, where d_0 is the initial mean diameter of the particles as deduced from the relationship between the PL energy and the QMC theory results.[4] To study the excitonic recombination energy for even smaller nanocrystal sizes, the sample with $d_0=3.2$ nm was reoxidized and re-etched. The PL spectrum and intensity of this twice-etched sample was less spatially homogenous relative to that of samples which had only been etched once, presumably due to etch-induced inhomogeneities. By selecting particular locations on the sample, regions with different PL peak energies and thus different inferred mean nanocrystal diameters could be probed. The spectra labeled $d_0=2.8$ nm and 2.5 nm in Fig. 2 were identified and probed using this approach. The exciting beam was focused on a fixed spot throughout each experiment so that any changes in PL for a single experiment were nominally due to changes within a given nanocrystal ensemble.

As shown in Fig. 2, for the $d_0=3.2$ and 2.9 nm samples, the emission energy increased monotonically with oxidation time in accord with expectations for a concomitant decrease in nanocrystal diameter. In contrast, for the two nanocrystal ensembles having the smallest d_0 values, the emission energy initially increased, but then began to decrease after ~7 min of oxidation.

The solid line in Fig. 3(a) shows the predictions of the QMC model of Puzder *et al.* for the emission energy of hydrogen-terminated Si nanocrystals as a function of their diameter.[4] When $d>\sim 3$ nm, this model predicts that surface states should have little effect on the excitonic recombination energy, and consequently, in this size regime, both hydrogen- and oxide-terminated nanocrystals should exhibit PL emission at their band gap energy. Monotonically increasing emission energies upon oxidation indicate that the $d_0=3.2$ and 2.9 nm samples fall in this size regime. The QMC model was then used in conjunction with the PL data of Fig. 2 to evaluate the nanocrystal diameter at each oxidation time by constraining the observed E_{max} (from Fig. 2) to the computational trend line of Fig. 3(a). The resulting deduced decrease in nanocrystal diameter as a function of air exposure time is plotted for the $d_0=3.2$ and 2.9 nm samples

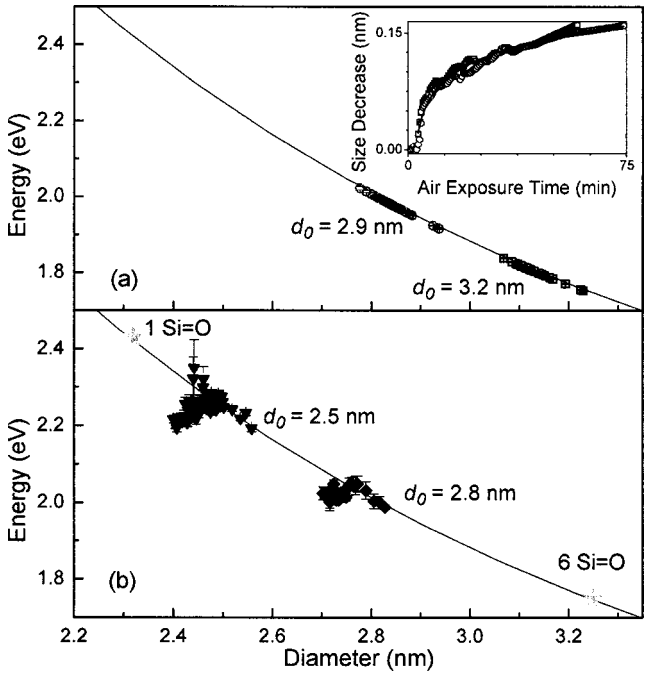

FIG. 3. Fit of data from Fig. 2 to QMC computations of Ref. 4 (solid line) for samples of Si nanocrystals with 2.5–3.2 nm initial diameters, d_0. (a) The nanocrystal emission energies are constrained to the computed curve for the emission energy of a silicon nanocrystal in the absence of surface states. The inset shows the relationship between size decrease and air exposure time derived from comparing the air exposure time in Fig. 2 to the sizes in Fig. 3(a). The solid line shows the fit to the size decrease, $\Delta d = 0.037 \cdot \ln(t - 1.70)$. (b) The nanocrystal samples' air exposure time is converted to size according to the relationship illustrated in the inset of (a). The stars represent the sizes at which, according to calculations, one and six Si=O double bonds, respectively, are required to introduce surface states.

in the inset of Fig. 3(a). The data are well-fitted by a logarithmic function, in accord with experiments on the time dependence of the room temperature growth of thin native oxide films on bulk Si surfaces.[13]

The emission energies of the smallest diameter nanocrystals clearly cannot be constrained to the calculated curve of Fig. 3(a), because the PL redshifted as the oxidation time increased (and presumably as particle size decreased). Instead, since the $d_0 = 2.8$ and 2.5 nm samples in Fig. 2 were oxidized similarly to the $d_0 = 3.2$ and 2.9 nm samples, all samples were assumed to have the same logarithmic oxidation kinetics. As shown in Fig. 3(b), for the initial period of oxidation, the observed PL energies followed the calculated curve for band-to-band emission, but once ~0.1 nm of Si had been converted to ~0.3 monolayers of silicon oxide, the emission energies were redshifted below the expected band gap. These data are consistent with the formation of an (oxygen-related) trap state in Si nanocrystals having $d_0 < 2.8$ nm. Surface strain can also lead to a decreased band gap in silicon nanocrystals,[14] but reflection high-energy electron diffraction measurements on these samples indicated that the nanocrystals were strain-free.

According to Refs. 3 and 4, below a certain diameter, a double-bonded surface group will introduce a deep-lying state that reduces the exciton recombination energy. One candidate for the oxygen-related state indicated by the data of Figs. 2 and 3 is therefore the Si=O bond. Formation of the Si=O bonds has been calculated to occur on a silicon surface by photoexcitation of Si–OH (an expected species due to water vapor in the air), with a barrier to formation of ~2.4 eV.[15] The 2.7-eV photons used for PL measurements could drive such a reaction process. The Si=O bond had also been observed by Fourier-transform infrared spectroscopy, as a metastable transient.[16] Indeed, observation of PL does not require a long-lived state as exciton lifetimes in Si nanocrystals at room temperature are 10–50 μs.[12]

Finally, we note that Puzder *et al.* have shown that while one Si=O bond will produce a defect level only for nanocrystal diameters below ~2.4 nm, multiple Si=O bonds will lead to the emergence of deep-lying states for large nanocrystal sizes. The star symbols in Fig. 3(b) indicate the minimum diameters at which one or six Si=O bonds are expected to produce a deep-lying state.[4] Since we observed a redshift in between these two extrema, only a small number of double-bonded surface species is theoretically required to have formed on our nanocrystals to produce the observed PL energy shifts.

In conclusion, the PL peak emission energy of Si nanocrystals with $d \sim 2.9$–3.4 nm shows an increase in excitonic recombination energy upon oxidation-induced size reductions, in agreement with calculations. For smaller nanocrystals ($d \sim 2.5$–2.8 nm), oxidation leads to an initial emission blueshift, but after the growth of ~0.3 monolayers of native oxide, a redshift is observed. The latter is consistent with the formation of an oxygen-related surface state. Selective etching of Si nanocrystal/SiO_2 composites leads to the formation of controlled ensembles of isolated nanocrystals that display oxidation kinetics similar to those of planar surfaces, making them available for future single-nanocrystal studies.

This work was supported by NSF. The Dutch contribution to this work is part of the research program of FOM and is financially supported by NWO.

[1] L. T. Canham, Appl. Phys. Lett. **57**, 1046 (1990).
[2] J. P. Proot, C. Delerue, and G. Allan, Appl. Phys. Lett. **61**, 1948 (1992).
[3] M. V. Wolkin, J. Jorne, P. M. Fauchet, G. Allan, and C. Delerue, Phys. Rev. Lett. **82**, 197 (1999).
[4] A. Puzder, A. J. Williamson, J. C. Grossman, and G. Galli, Phys. Rev. Lett. **88**, 097401 (2002).
[5] S. Schuppler, S. L. Friedman, M. A. Marcus, D. L. Adler, Y.-H. Xie, F. M. Ross, Y. J. Chabal, T. D. Harris, L. E. Brus, W. L. Brown, E. E. Chaban, P. F. Szajowski, S. B. Christman, and P. H. Citrin, Phys. Rev. B **52**, 4910 (1995).
[6] Y. Kanemitsu, H. Uto, Y. Masumoto, T. Matsumoto, T. Futagi, and H. Mimura, Phys. Rev. B **48**, 2827 (1993).
[7] L. Pavesi, L. Dal Negro, C. Mazzoleni, G. Franzo, and F. Priolo, Nature (London) **408**, 440 (2000).
[8] M. H. Nayfeh, S. Rao, N. Barry, J. Therrien, G. Belomoin, A. Smith, and S. Chaieb, Appl. Phys. Lett. **80**, 121 (2002).
[9] J. F. Ziegler, J. P. Biersack, and U. Littmark, *The Stopping and Range of Ions in Solids* (Pergamon, New York, 1985).
[10] K. S. Min, K. V. Shcheglov, C. M. Yang, H. A. Atwater, M. L. Brongersma, and A. Polman, Appl. Phys. Lett. **68**, 2511 (1996).
[11] J. Valenta, R. Juhasz, and J. Linnros, Appl. Phys. Lett. **80**, 1070 (2002).
[12] M. L. Brongersma, A. Polman, K. S. Min, E. Boer, T. Tambo, and H. A. Atwater, Appl. Phys. Lett. **72**, 2577 (1998).
[13] F. Lukeš, Surf. Sci. **30**, 91 (1972).
[14] N. Daldosso, M. Luppi, S. Ossicini, E. Degoli, R. Magri, G. Dalba, P. Fornasini, R. Grisenti, F. Rocca, L. Pavesi, S. Boninelli, F. Priolo, C. Spinella, and F. Iacona, Phys. Rev. B **68**, 085327 (2003).
[15] F. Zhou and J. D. Head, J. Phys. Chem. B **104**, 9981 (2000).
[16] Y. J. Chabal, K. Raghavachari, X. Zhang, and E. Garfunkel, Phys. Rev. B **66**, 161315(R) (2002).